

Electronic Supplementary Information

Room Temperature Formation of Organic-Inorganic Lead Halide Perovskites: Design of Nanostructured and Highly Reactive Intermediates

Hong Zhang, ^a Dan Li, ^c Jiaqi Cheng, ^a Francis Lin, ^b Jian Mao, ^a Alex K.-Y. Jen,^b Michael Grätzel ^d and Wallace C.H. Choy^{*,a}

^a Department of Electrical and Electronic Engineering, The University of Hong Kong, Pok Fu Lam Road, Hong Kong, China. E-mail: chchoy@eee.hku.hk

^b Department of Materials Science & Engineering, University of Washington, Seattle, Washington 98195, United States.

^c Key Laboratory of Luminescence and Optical Information, Ministry of Education, School of Science, Beijing Jiaotong University, Beijing 100044, China.

^d Laboratory for Photonics and Interfaces, Institute of Chemical Sciences and Engineering, School of Basic Sciences, Ecole Polytechnique Fédérale de Lausanne, CH-1015 Lausanne, Switzerland.

Table S1. The basic chemical properties of different ligands.

Ligand	van der Waals Volume (cm ³ . mol ⁻¹) ^a	Boiling point (°C)	PbI ₂ solubility (mg/ml) ^b	PbI ₂ .(L) _x conversion time (s) ^c	PbI ₂ /L coordination ratio ^d	Interlayer spacing of PbI ₂ .(L) _x (Å)
-	-	-	-	-	-	6.918 ^e
TBP	146.05	197	148	300	1:1	15.152
Py	79.89	115	<5	100	1:2	8.598
DMF	77.52	153	475	50	1:1	9.196
DMSO	71.43	189	595	140	1:2	8.437
EDA	68.82	116	<5	50	1:2	-

a) <http://www.molinspiration.com/cgi-bin/properties>. b) The solubility test was conducted at room temperature (25 °C). c) The progress of chemical reactions was monitored by UV-vis spectra. d) The data were estimated by TGA. e) The interlayer spacing of

Thermogravimetric analysis (TGA)

The content of L in the $\text{PbI}_2 \cdot (\text{L})_x$ complexes were estimated by TGA. The TGA results of $\text{PbI}_2 \cdot (\text{L})_x$ intermediates were shown in **Figure S1**. The $\text{PbI}_2 \cdot (\text{Py})_2$ and $\text{PbI}_2 \cdot \text{DMF}$ complexes exhibited a one-step decomposition process with weight-loss of 25.41% and 13.34% at 135.49°C and 113.11°C, respectively. $\text{PbI}_2 \cdot (\text{DMSO})_2$ intermediate exhibited a two-step decomposition process with weight-loss of 12.40% at each step and was completely decomposed at 142.59°C. Both $\text{PbI}_2 \cdot (\text{EDA})_2$ and $\text{PbI}_2 \cdot \text{TBP}$ intermediate also shown a two-step decomposition process and completely decomposed at 328.72°C and 263.71°C with weight-loss of 19.72% and 23.0%, respectively. The value of x is calculated as follows:

$$x = \frac{M_w(\text{PbI}_2) \times W_{\text{loss}}\%}{M_w(\text{L})(1 - W_{\text{loss}}\%)} \quad (1)$$

where $M_w(\text{PbI}_2) = 461$ g/mol, $M_w(\text{L})$ is the molecular weight of ligand, $W_{\text{loss}}\%$ is refer to the weight proportion of ligand in the $\text{PbI}_2 \cdot (\text{L})_x$ intermediates. Then, we can get the content of L in the $\text{PbI}_2 \cdot (\text{L})_x$ intermediates as we summarized in **Table S1**.

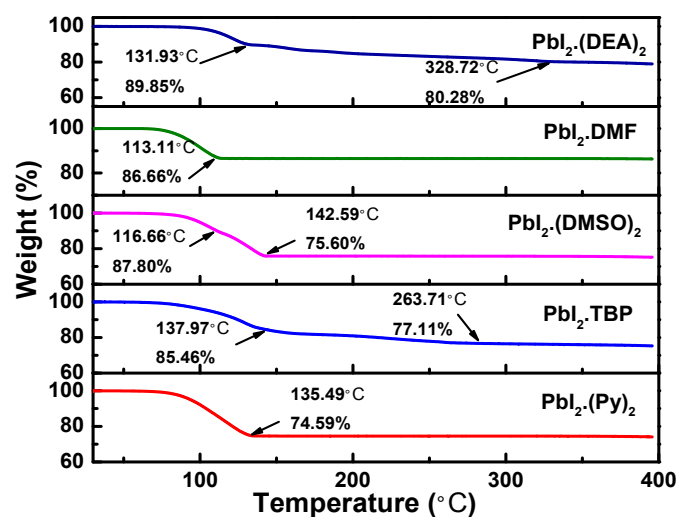


Figure S1. Thermogravimetric analysis (TGA) of $\text{PbI}_2 \cdot (\text{L})_x$ intermediates.

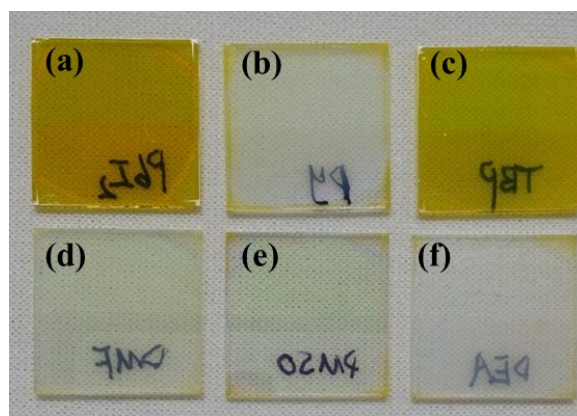


Figure S2. The photographs of $\text{PbI}_2(\text{L})_x$ intermediates in which (a) is PbI_2 , (b) is $\text{PbI}_2(\text{Py})_2$, (c) is $\text{PbI}_2.\text{TBP}$, (d) is $\text{PbI}_2.(\text{DMSO})_2$, (e) is $\text{PbI}_2.\text{DMF}$, and (f) is $\text{PbI}_2.(\text{DEA})_2$ film.

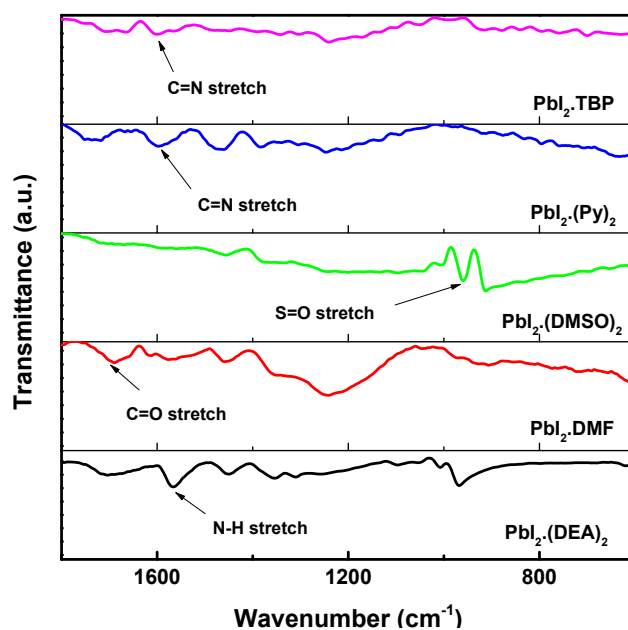


Figure S3. Fourier transform infrared spectrometer (FTIR) of $\text{PbI}_2(\text{L})_x$ complexes.

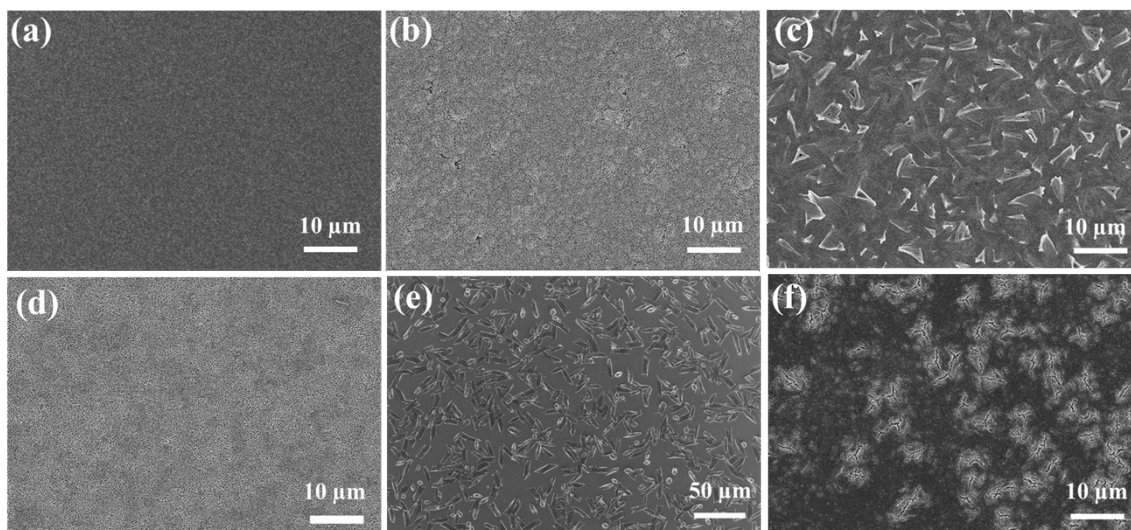


Figure S4. Top-view SEM images of $\text{PbI}_2(\text{L})_x$ intermediates with low magnification in which (a) is untreated PbI_2 , (b) is $\text{PbI}_2(\text{Py})_2$, (c) is PbI_2TBP , (d) is $\text{PbI}_2(\text{DMSO})_2$, (e) is PbI_2DMF and (f) is $\text{PbI}_2(\text{EDA})_2$ film.

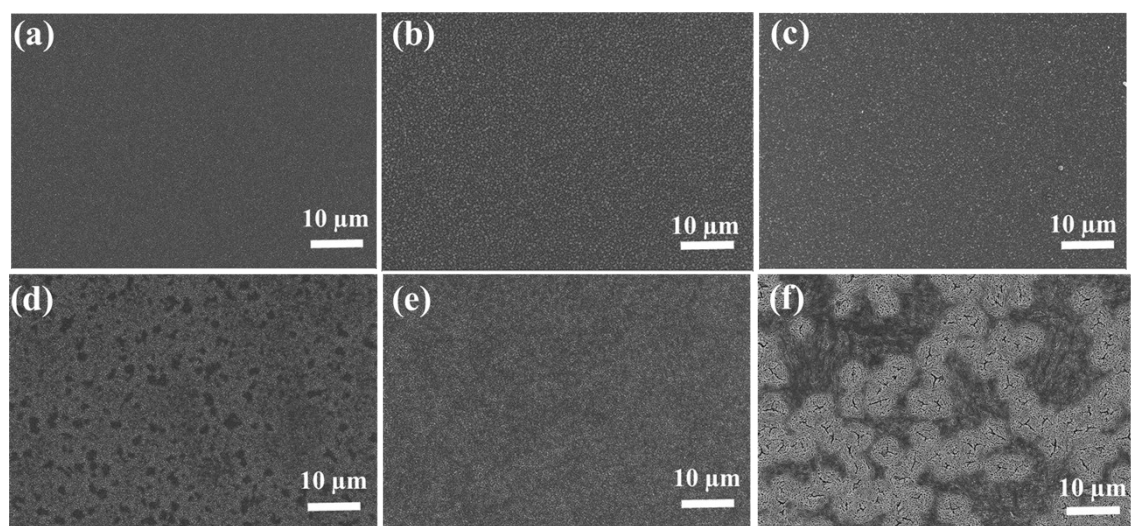


Figure S5. Top-view SEM images of $\text{CH}_3\text{NH}_3\text{PbI}_3$ films with low magnification from (a) PbI_2 , (b) $\text{PbI}_2(\text{Py})_2$, (c) PbI_2TBP , (d) $\text{PbI}_2(\text{DMSO})_2$, and (e) PbI_2DMF on NiO_x/ITO substrate. (f) Top-view SEM image of $\text{PbI}_2(\text{EDA})_2$ film after dipping into $\text{CH}_3\text{NH}_3\text{I}$ solution with low magnification.

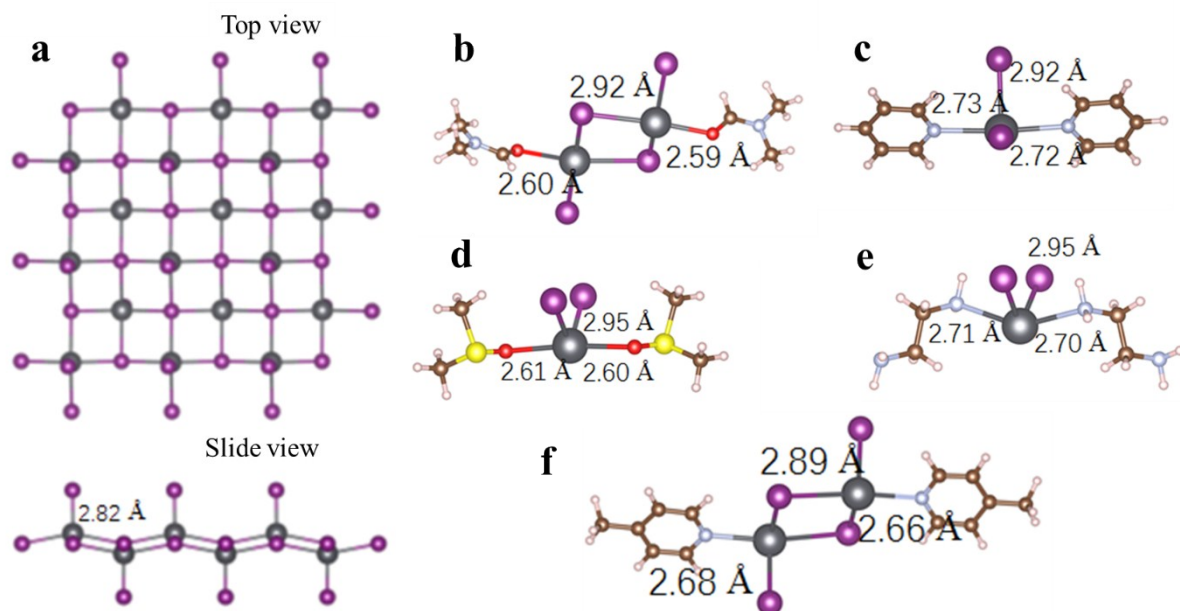


Figure S6. Crystallographic structures of PbI_2 (a), $\text{PbI}_2\cdot\text{DMF}$ (b), $\text{PbI}_2\cdot(\text{Py})_2$ (c), $\text{PbI}_2\cdot(\text{DMSO})_2$ (d), $\text{PbI}_2\cdot(\text{EDA})_2$ (e), and $\text{PbI}_2\cdot\text{TBP}$ (f).

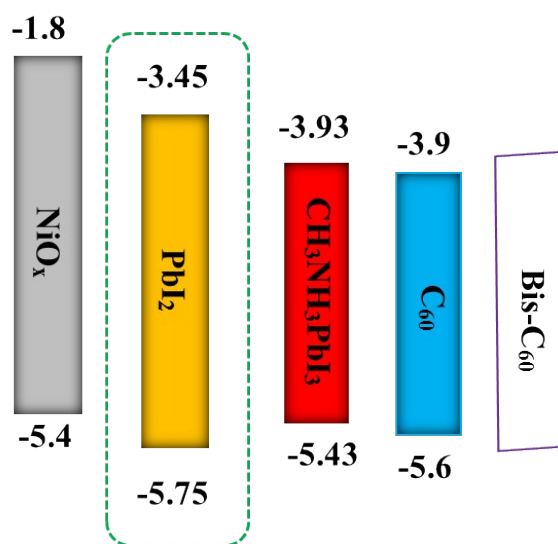


Figure S7. Energy diagram of each material in the PVSC device, with energy levels given in eV.